

SC/66a/RMP/5

A new variance estimator for Northeast Atlantic minke whales applied to survey data from 1996-2001.

Hans J. Skaug, Hiroko K. Solvang



INTERNATIONAL
WHALING COMMISSION

Measurement error model for the Norwegian minke whale surveys 2008-2013

Hiroko K. Solvang, Hans J. Skaug, Nils Øien

Institute of Marine Research, P.O.Box 1870 Nordnes, N-5817 Bergen, Norway

hiroko.solvang@imr.no

ABSTRACT

A discrete approximation to model the measurement error for the estimation of radial distance and angle to detect objects in the line transect surveys is presented. This approach is to directly calculate the effect of measurement error on the effective strip half width. The measurement error for the experimental data collected over the period 2008-2013 is explored. These results indicate that the abundance estimates taking into account the measurement error are larger than the abundance estimates without any measurement error correction.

KEYWORDS: EFFECTIVE STRIP HALF-WIDTH, ABUNDANCE ESTIMATION, DISCRETE MIXTURE MODEL, LIKELIHOOD

INTRODUCTION

The Norwegian minke whale surveys use a double platform design in which the radial distance and sighting angle are estimated by eye for each surfacing of a whale (Skaug et al. 2004). Separate distance and angle experiment are routinely conducted as part of the surveys with the aim to estimate bias and variability of the measurement error (Bøthun et al. 2008). A simulation based correction method has been applied previously to the abundance estimates (Skaug et al. 2004). The simulation procedure also accounted for other factors, such as errors in duplicate identification, but the isolated effect of distance and angle measurement error was never quantified. In the present paper we use an approach for errors formed as multiplicative of observation and true values introduced in Marques (2004) and Borchers et al. (2010). The multiplicative errors model might be appropriate when the error tend to increase with the original distance/angle. We calculate the effect of measurement error on the effective strip half width. Measurement error in distance is often ignored in line transect analysis. Marques (2004) defined the distribution of the observed distances with error that were described by continuous distributions. On the other hand, Borchers et al. (2010) reviewed this literature and propose correction to the likelihood that accounts for measurement error. We adopt a similar approach, but for computational simplicity we use discrete measurement error models. A complication arises for our minke whale surveys due to the double platform design and the non-standard survey protocol (see below).

EXPERIMENTAL DATA

The distance and angle experiments are conducted by using two buoys as target objects under sighting conditions representative for the ordinary survey activity. These buoys are dropped into the sea at distances of 1000 to 4000 meters from the vessel. The vessel then moves towards the buoys at a speed between 6 and 10 knots at different courses. On a signal from the cruise leader the observer provides a momentarily estimate of the angle and distance to the buoy. At the same time the true values are recorded by the ships radar operator. All measurements are recorded in the same way as during the survey. This procedure is repeated several times as the vessel approaches the buoys. Since several recordings are made within each drop of the buoys, one expects the data to be positively serial correlated. The cruise leader switches between the buoys at random and the vessel also changes the course several times during the approach towards the buoys to reduce this serial correlation. After having tested one observer, the vessel moves away from the buoys and a new observer is tested following the same procedure. In this way a series of about 10 readings is generated together with a calibration curve for each trial. In the analyses presented here for the 2008-2013 survey period, data from four participating vessels have been used; these data include 524 observations for distance from platform 1 and 541 observations from platform 2, while there are 532 and 550 angle observations from platform 1 and platform 2, respectively.

MEASUREMENT ERROR MODEL

Consider first a single platform, and denote by r_t and r_o the true and recorded (observed) radial distance, respectively. For each individual observation we refer to errors of the form observed = true \times error as multiplicative and calculate the error as $c^{(r)} = r_t / r_o$, and hence $c^{(r)} = 1$ means no error ($r_t = r_o$). Similarly we define θ_t (true sighting angle), θ_o (observed sighting angle), and $c^{(\theta)} = \theta_t / \theta_o$. Although it is the joint probability density of (r_o, θ_o) that is needed for the likelihood we will start with the marginal density of r_o .

Under the expression for the distribution of the observed distance shown in Marques (2004), we have the following probability density function (pdf)

$$f_o(r_o) = \int f_t(r_t) f_c(c^{(r)}) dc^{(r)} \quad (1)$$

where $f_t(r_t)$ is the probability density of the true distances, and as a mathematical expression for $f_t(r_t)$ we use the marginal of eqn (2) in Skaug et al (2004). The latter is the bivariate density of the location of the initial position of a sighted whale, cast in Cartesian coordinates. By transforming to polar coordinates we obtain both $f(r_t)$ (and $f(\theta_t)$) as marginal densities of the joint density eqn. (2) in Skaug et al. (2004). When inserted $r_t = c^{(r)} \times r_o$ into (1), this yields

$$f_o(r_o) = \int f_t(c^{(r)} r_o) f_c(c^{(r)}) c^{(r)} dc^{(r)}, \quad (2)$$

which is easily seen corresponds to each term of the formula represented in Marques (2004).

Marques (2004) and Borchers et al. (2010) assumed continuous distributions for errors. For computational simplicity, we assume a discrete distribution to errors. The real values of the discrete random variable is given by distinct values $c_1^{(r)}, \dots, c_i^{(r)}, \dots, c_k^{(r)}$ and $f_t(c^{(r)} r_o)$ is replaced by $f(c_i^{(r)} r_o)$. Therefore, the discrete density expression for eq.(2) is given by

$$f_o(r_o) = \sum_{i=1}^k c_i^{(r)} p(C = c_i^{(r)}) I_{\{c_i^{(r)}\}}(C) \times f_t(c_i^{(r)} r_o) \quad (3)$$

where $I_{\{c_i^{(r)}\}}(C) = 1$ if $C = c_i^{(r)}$ and $I_{\{c_i^{(r)}\}}(C) = 0$ if $C \neq c_i^{(r)}$. Furthermore, we assume that $p(C = c_1^{(r)}) + \dots + p(C = c_k^{(r)}) = 1$ under the pair of error and the probability $(c_i^{(r)}, p(C = c_i^{(r)}))$ for $i = 1, \dots, k$. That is, eq.(3) also expresses a discrete mixture distribution model.

In order to construct the likelihood function from Skaug et al (2004) we need the joint probability of (r_o, θ_o) , which equivalent to (2) is

$$f(r_o, \theta_o) = \sum_{i=1}^k c_i^{(r)} p^{(r)}(C = c_i^{(r)}) \times c_i^{(\theta)} p^{(\theta)}(C = c_i^{(\theta)}) \times f_t(c_i^{(r)} r_o, c_i^{(\theta)} \theta_o).$$

where $f_t(r_i, \theta_i)$ is given as the product of (2) and (5) in Skaug et al (2004), where a double platform version of (2) is used, i.e. (4) in Skaug et al 2004 is used.

In this study, the discrete error model for $c^{(r)} = r_i / r_o$ (and $c^{(\theta)} = \theta_i / \theta_o$) is assumed to be assigned into three classes, that is, $k = 3$ and $p(C = c_1^{(*)}) + p(C = c_2^{(*)}) + p(C = c_3^{(*)}) = 1$. $p(C = c_1^{(*)})$ and $p(C = c_3^{(*)})$ indicate the probabilities for measurement error around true values and p_2 is a probability for the region taken as true value. The threshold to detect three classes involved 10, 20, 25, 30% quantile points. For 10% quantile points, $p(C = c_1^{(*)})$, $p(C = c_3^{(*)})$ and $p(C = c_3^{(*)})$ indicate 10, 80, 10%. If we don't assume any measurement error, $p(C = c_1^{(*)}) = p(C = c_3^{(*)}) = 0\%$ and $p(C = c_2^{(*)}) = 100\%$. The error values $c_1^{(*)}$, $c_2^{(*)}$ and $c_3^{(*)}$ are calculated as the representative values for three classes by taking the average within each class.

RESULTS

Histograms for the errors c_i of radial distance and angle are shown in Figs.1 and 2, respectively. The ratio for radial distance presented slightly different distributions depending on Vessels, e.g. ERO and JHJ. Those cases also indicate a bit difference between the two platforms. Vessel THO

includes outliers for platform 2 (CV of platform 2 is larger than CV of platform 1) that are not shown in the figure. The distributions for the angle ratios were mostly centered around 1. However, the data for HGU showed a large deviation (skewed to the left) from 1.

Using the probabilities for measurement error measured at experiments conducted on all vessels, we calculated the effective strip half-widths based on statistical methods for abundance estimation performed in Skaug et al. (2004). The results are summarized in Table 1 in addition to expected values of the ratio and coefficient of variation for distance and angle for each platform and average for both platforms. In the table, the effective strip half-widths were for one platform. For the main abundance estimation assuming no measurement error, the effective strip half-widths are calculated to 280.3 meters. On the other hand, the effective strip half-widths with 10-30% measurement error were less than 280.3 meters. Furthermore, if we assume measurement error for only distance or only angle, those effective strip half-widths were 251.8 meters and 264.7 meters, respectively (these values are not shown in Table1).

DISCUSSIONS

The abundance estimates are inversely proportional to the effective strip half-widths. Since the effective strip half-widths including measurement error always become less than the ones assuming no measurement error, those estimates become larger than any case where measurement error has not been taken into account. That is, the measurement error uncorrected abundance estimate always becomes the minimum estimate as compared to estimates involving any measurement error corrections. The effective strip half-widths tend to decrease as measurement error is incorporated. This means that the abundance estimates without bias correction for measurement error are conservative estimates. This tendency was consistent with the experiments for the survey period 1996-2001.

We assumed a multiplicative error model for measurement errors for both distance and angle in this study. On the other hand, the resulting error associated with a given angle may not tend to be proportional to the original true angle and an additive error model could be more appropriate in that case than a multiplicative model.

REFERENCES

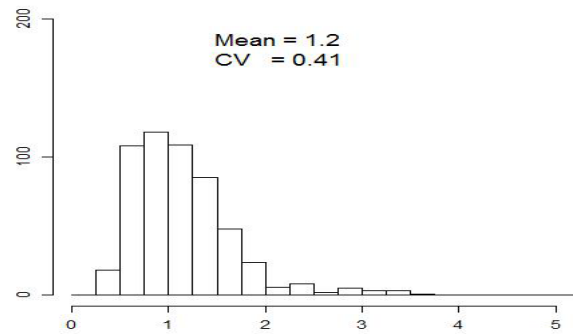
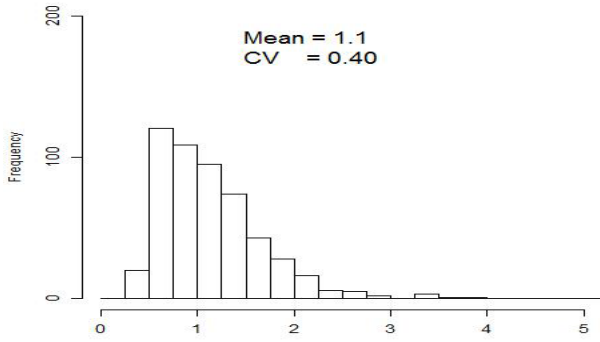
- Skaug, H.J., Øien, N., Schweder, T. and Bøthun, G. 2004. Abundance of minke whales (*Balaenoptera acutorostrata*) in the Northeast Atlantic: variability in time and space. *Canadian Journal of Fisheries and Aquatic Sciences*, 61:870-886.
- Marques, T.A. 2004. Predicting and correcting bias caused by measurement error in line transect sampling using multiplicative error models. *Biometrics* 60:757-763.

- Borchers, D.T. Marques, T. Gunnlaugsson and P. Jupp. 2010. Estimating Distance Sampling Detection Functions When Distances Are Measured With Errors. *Journal of Agricultural, Biological, and Environmental Statistics* **15**(3): 346-361.
- Bøthun, G., Øien, N. and Skaug, H.J. Measurement error in survey and experiment, Norwegian minke whale surveys 2002-2007. *SC/60/PFI5, IWC Scientific Committee, May 2008.*
- Skaug, H.J. Simplification of the estimation procedure for Norwegian minke whale surveys. *SC/65b/RMPWP01, IWC Scientific Committee, May 2014.*

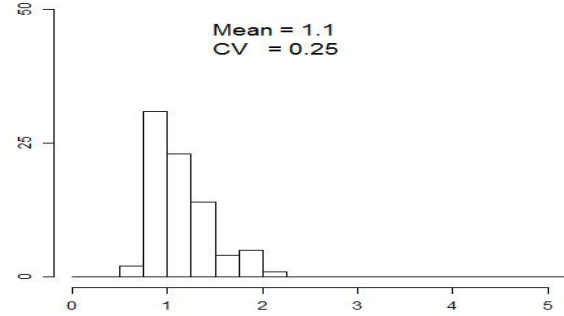
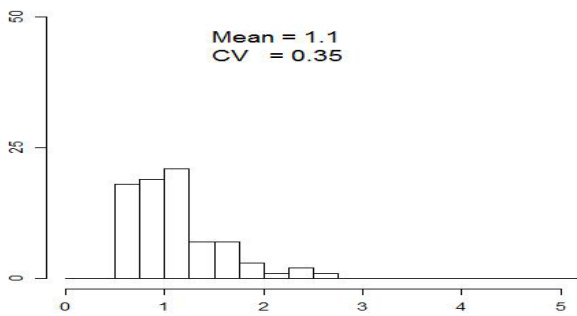
PLATFORM 1

PLATFORM 2

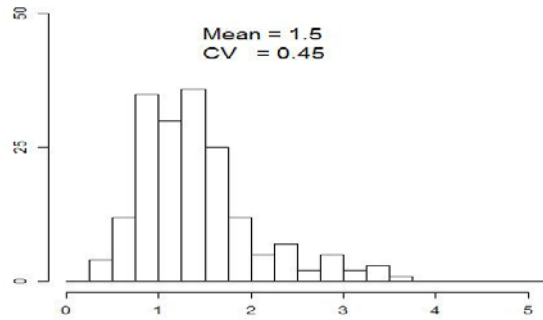
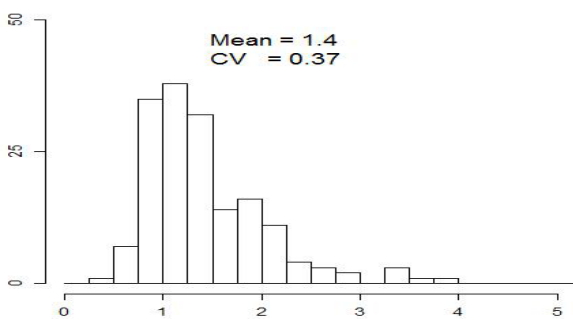
4 vessels



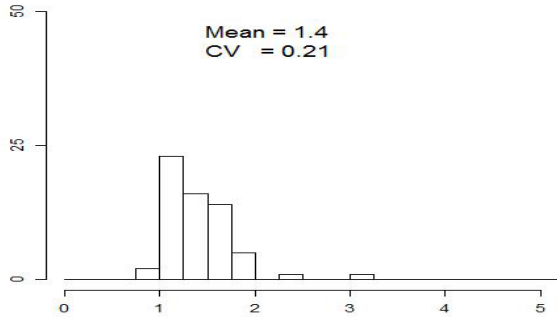
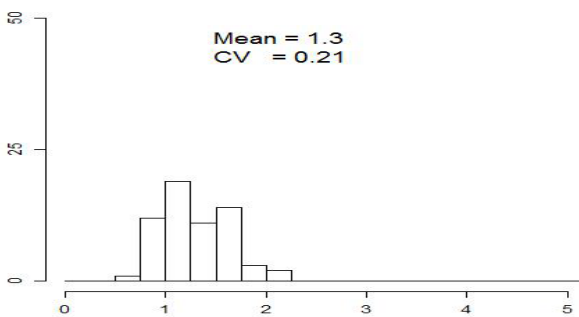
ERO



THO



JHJ



HGU

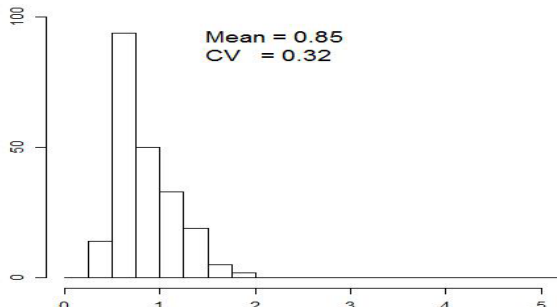
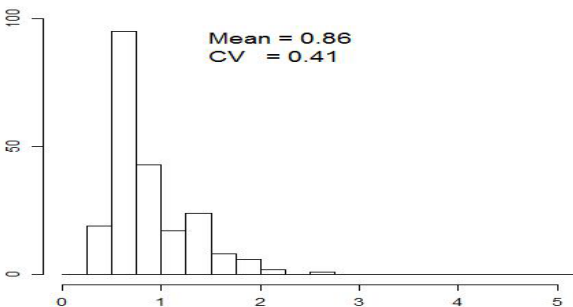
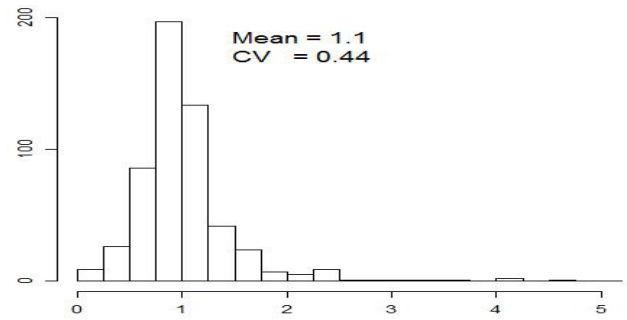
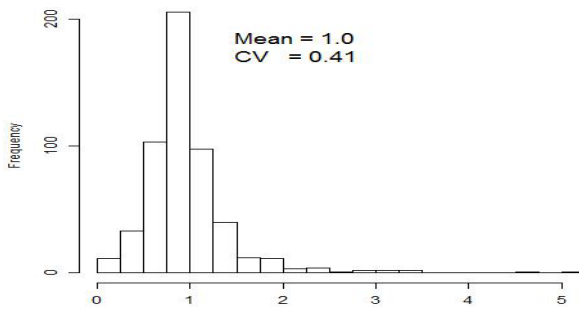


Fig. 1. Histograms of the ratios for the radial distance's measurement error. Those for platforms 1 and 2 are on the left and right side. The top histograms are given by the data aggregating four vessels. Mean and CV are obtained based on dividing measurement error into three classes based on the quartile (25%).

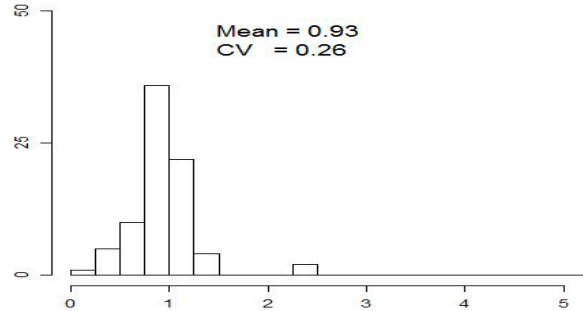
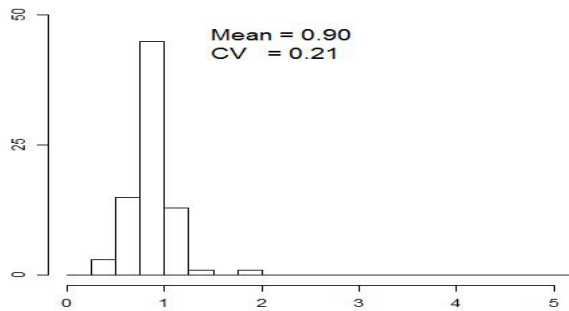
PLATFORM 1

PLATFORM 2

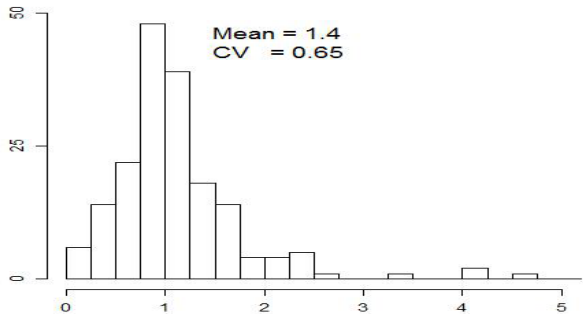
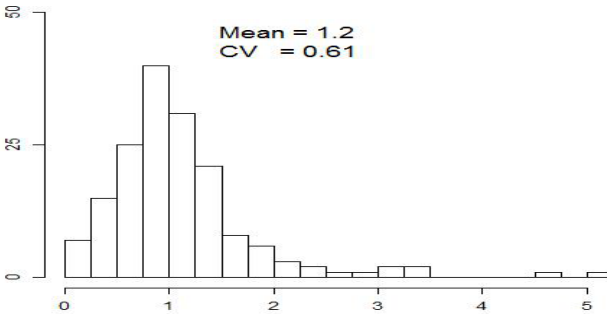
4 vessels



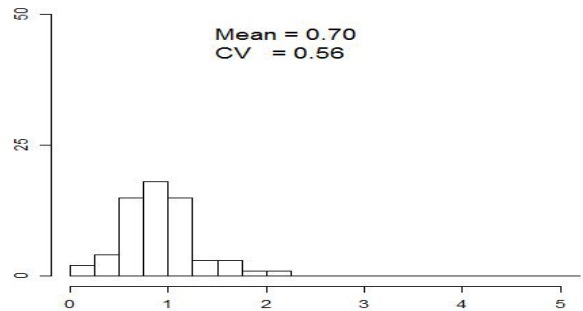
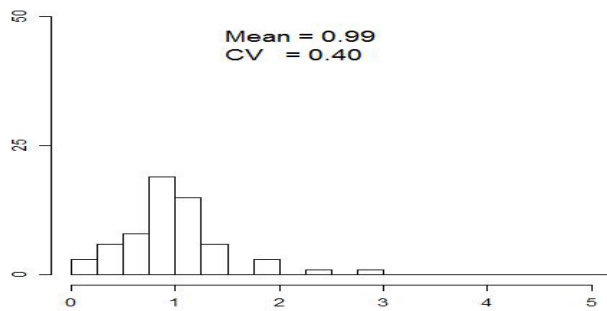
ERO



THO



JHJ



HGU

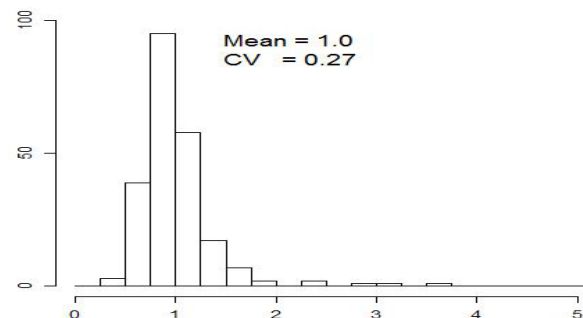
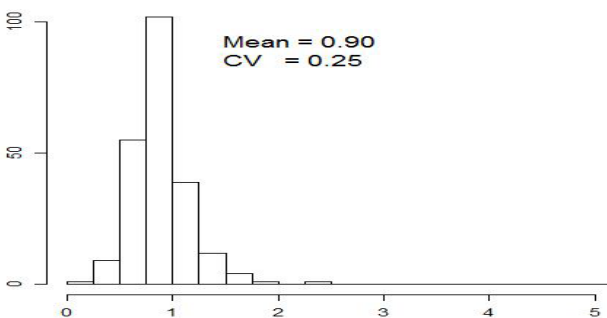


Fig. 2. Histograms of the ratios for the angle's measurement error. Those for platforms 1 and 2 are on the left and right side. The top histograms are given by the data aggregating four vessels. Mean and CV are obtained based on dividing measurement error into three classes based on the quartile (25%).

Table 1. Probabilities (p_1, p_2 and p_3) for three categories of measurement error, the effective strip half-widths (e.s.h.w), expected value of the error (Mean c) and coefficient of variation (CVc) for distance (r) and angle (t) in the cases of each platform and average for both platforms.

ME data	p_1	p_2	p_3	e.s.h.w	Distance (r)		Angle (t)	
					Mean c	CVc	Mean c	CVc
No ME	0%	100%	0%	280.3	1.1	0	1	0
Platform1	10%	80%	10%	237.7	1.1	0.37	1.0	0.48
	20	60	20	216.8	1.1	0.40	1.0	0.44
	25	50	25	197.4	1.1	0.40	1.0	0.41
	30	40	30	194.6	1.1	0.40	1.0	0.39
Platform2	10%	80%	10%	253.4	1.2	0.41	1.1	0.54
	20	60	20	235.9	1.2	0.42	1.1	0.46
	25	50	25	227.3	1.2	0.41	1.1	0.44
	30	40	30	224.0	1.2	0.40	1.1	0.41
Average of platforms 1 and 2	10%	80%	10%	244.7	1.2	0.39	1.1	0.51
	20	60	20	227.6	1.2	0.41	1.1	0.45
	25	50	25	216.9	1.2	0.41	1.1	0.42
	30	40	30	211.8	1.2	0.40	1.1	0.4